Preparation of ordered Ag@Au hybrid nanotubes arrays and their fluorescence enhancement of poly(3-hexylthiophene)

Wang Jianchao (wangjc5670@163.com)
Jishou University https://orcid.org/0000-0002-8488-1903
Gege Tang
Jishou University
Huayong Peng
Jishou University

Nano Express

Keywords: galvanic displacement reaction, ordered Ag@Au hybrid nanotubes, poly(3-hexylthiophene), fluorescence enhancement

Posted Date: April 1st, 2021

DOI: https://doi.org/10.21203/rs.3.rs-370802/v1

Abstract

The ordered silver nanowires (Ag NWs) were assembled by three-phase interface method and the ordered Ag@Au hybrid nanotubes were successfully prepared by the galvanic replacement reaction between $HAuCl_4$ solution and the ordered Ag NWs. Field emission scanning electron microscope (FESEM) and transmission electron microscope (TEM) were employed to analyze the morphology of the ordered Ag NWs and Ag@Au nanotubes, and the influence of reaction time in displacement reaction. Fluorescence and laser-Raman properties of conjugated polymerpoly(3-hexylthiophene) (P3HT) were analyzed on various ordered Ag@Au nanotubes on the fluorescence. The results showed that the Au particle grew on ordered Ag@Au hybrid nanotubes with the reaction time going. The fluorescence properties of P3HT films are improved on various ordered Ag@Au hybrid nanotubes compared with those on bare silicon substrate, but the fluorescence intensity of P3HT films on the ordered hybrid nanowires decreases as the galvanic displacement process.

Introduction

Over the past 30 years, fluorescence has become the dominant detection/sensing technology in medical diagnostics and biotechnology. Although fluorescence is a highly sensitive technique, there is still a driving force for reduced detection limits further. Metal-enhanced fluorescence (MEF) is an increase in the fluorescence of a fluorophore when it is in close to a metallic nanostructure, which can enhance the local field of the fluorophore. Due to the electromagnetic coupling between the fluorophore and the metal nanoparticles, the excitation rate increases, the fluorescence quantum yield increase, the lifetime reduce and the photostability of fluorescent groups improve. MEF effects greatly depend on the structure of the substrates. The periodic metal nanostructures arrays could greatly improve electric field and the enhancement factor, and improve the fluorescence intensity and photostability of fluorescent groups. The future of MEF in biotechnology and life science will depend on the extensive development of advanced micro/nano technology and electromagnetic modeling.

At present, various metal nanoarrays have been used as MEF substrates, such as nanowires, nanorods, nanopores, nano triangular prisms, etc. Silver nanowires (Ag NWs) are an ideal candidate for large surface areas and high crystallinity for metal fluorescence enhancement [1, 2]. However, surface plasmon resonance peaks are fixed at about 350 to 377 nm. Surface plasmon resonance wavelength of Ag NWs is far away from most emission wavelength of fluorophore, thus limiting their application as reproducible and ultrasensitive sensing platforms. Ag NWs with a broad range of surface plasmon resonance are highly desirable. Introducing a second metal into Ag NWs and adjusting the content can change the substrate plasmon resonance characteristics. However, there are few reports about bicomponent ordered metal nanowire arrays as fluorescence enhancement substrates and the effect of the interaction between the two components on the fluorescence properties. Gold nanopaticles (Au NPs) have characteristic surface plasmon resonance peaks in the wavelength range λ = 530-545 nm, matching with emission wavelength of fluorophore dyes, thus Ag@Au hybrid nanotubes is designed and synthetized.

Preparation methods of metal nanotubes usually include the synthesis of metal nanoparticles from salt precursors on surface of nanowire templates [3,4], and subsequent etching [5]. Silicon nanowire, anodic alumina (AAO), and organic tubular is commonly used as templates [6, 7]. Using the template methods, the shape and structure are easy to control, and various complex structures such as core-shell hybrid materials can be synthesized. After etching, the order of the template is usually destroyed. The sacrificial template method is another method to prepare of metal nanotube structure, in which the solid template is replaced by other materials during galvanic displacement reaction. In the reaction, the metal template with lower reduction potential is used as sacrificial template, and then template shape-like metal structure with higher reduction potential or bimetallic nano structure can be obtained. Silver nanostructures have been used as sacrificial templates to prepare other porous metals and metal oxide structures. Xia et al. have reported a lot of work on shape or shape controlled nanostructures, such as cubes, spheres and other porous structures [8-13].

Recently, we have expanded the traditional displacement reaction method to prepare ordered Ag@Au hybrid nanotubes arrays. Although many studies have reported the synthesis of various porous structures, there are few studies on the ordered Ag@Au hybrid nanotubes arrays. In this paper, the synthesis and reaction rate of gold nanotubes using sacrificial Ag NWs as template were studied. The reaction process can be controlled by controlling the reactant concentration and reaction time. In addition, the conjugated polymer poly (3-hexylthiophene) (P3HT) was used as fluorescent probe to investigate the different MEF effect on ordered Ag@Au hybrid nanotubes arrays.

Methods

1.1 Reagents

Ag NWs (10 mg/mL) aqueous solution was purchased from Sino-Platinum Metals Co. Ltd., China. Gold(III) chloride trihydrate($AuCl_3$•HCl•$4H_2O$) was purchased from Tianjin meisco Chemical Co., Ltd, China. P3HT (Mw = 30 kg/mol) was purchased from Shanghai Aladdin Biochemical Technology Co., Ltd, China. All chemicals except for special instructions were analytical grade and used without further purification. Milli-Q deionnized water (resistivity >18.0M cm-1) was used for all preparations.

1.2 Fabrication of ordered Ag nanowire arrays

Five milliliters of AgNWs aqueous suspension was added to the liquid surface of 25 mL chloroform in a glass vessel. An interface was formed among two immiscible liquids. One milliliter of acetone was added cautiously and dropwise to the mixture. Minutes later, a sparkling mirror-like surface emerged. The ordered Ag nanowire films were then transferred onto silicon chips and dried at room temperature. The sample was labeled as S0.

1.3 Preparation of ordered Ag@Au hybrid nanotube arrays

As shown in Scheme, Ag nanowire arrays was immersed in 1 mM $HAuCl_4$ solution for a certain time (2.5, 5, 10, 30 min) to obtain Ag @ Au hybrid nanotube arrays. Then, the as-fabricated substrates with ordered Ag @ Au hybrid nanotubes were washed with water several times to remove the residual $HAuCl_4$. Finally, these films were dried at room temperature. The sample was labeled as S1, S2, S3, S4.

1.4 Spin coating P3HT film

Thirty microliters of P3HT/chlorobenzene solution with the concentration of 5 mg/mL was added to the nanowire or nanotube arrays, and then spin-coated at 2000 rpm for 60 s. To further remove the residual solvents, the samples were kept in a dark environment for at least 12 h after spin-coating. All the above procedures were carried out at room temperature.

1.5 Characterization

The synthesized Ag NWs and gold nanotubes were investigated using field emission scanning electron microscopy (JSM- 7001F, JEOL) and transmission electron microscopy(HT7700, HITACHI). UV-Vis absorption spectra were obtained (UV-2600, Shimadzu) before and after the replacement reaction. PL spectra were measured on a fluorescence spectrometer (FP-8300 JASCO fluorescence spectrometer). For the steady-state measurements, the samples were excited by a Xe lamp at 557 nm. The Raman spectroscopy was performed on a HORIBA LabRAM HR800 micro-Raman spectrometer equipped with an Ar ion laser as the excitation source (633 nm), and the spectra were obtained within 5 s of exposure.

Results And Discussion

2.1 Morphology of ordered Ag nanowires and Ag@Au hybrid nanotubes

2.1.1 Scanning electron microscopy

Fig. 2-a show the ordered Ag NWs prepared by the three-phase interface method, and fig. 2-b is an enlarged view. Through the three-phase interface method, the disordered Ag NWs can be self-assembled to large-area ordered Ag NWs, with mooth surface, nanowires parallel and closely connected to each other. The silver wire is the electron source and template for gold nanotube. Fig. 2c -l are scanning electron microscope images of the Ag@Au hybrid nanotubes by galvanic replacement reaction. During the replacement reaction, the gray silver nanowire substrare turns brown, indicating the formation of Au nanoparticles. Fig. 2c-g shows the morphology of ordered Ag@Au nanotubes were prepared by ordered Ag NWs reacting with 1 mM $HAuCl_4$ solution for different times (2.5, 5, 10, 30min) respectively. As shown in Fig. 2, Au NPs formed on the surfaces of Ag NWs by the galvanic displacement reaction between Ag and $AuCl_4$- for different times. With time going on, the layer of Au nanoparticles grow thicker. The incorporation of Au NPs onto the surface of Ag NWs forms mesoporous and hollow tube-like structure. The surface of the nanowires becomes rough, and a lot of nanoparticles are gradually formed. It was observed that the size and density of Au nanopaticles increases with the extension of reaction time, SEM showed that the gold layer on the surface of Ag NWs was synthesized, forming continuously and the

porous gold nanotubes. The reason for the formation of gold nanoparticles was that the standard reduction potential of the Ag+/Ag pair (0.80 V vs. standard hydrogen electrode, SHE) is lower than that of the $AuCl_4$-/Au pair (0.99 V vs. SHE).

2.1.2 Transmission electron microscopy of Ag NWs and Ag@Au hybrid nanotubes

Fig. 3 shows TEM images of Ag NWs reacting with 1 mM $HAuCl_4$ solution for different times. It can be seen that the surface of Ag NWs is smooth and uniform, the diameter is about 120 nm. After reacting with 1 mM $HAuCl_4$, the surface of Ag NWs is corroded with the extension of reaction time. Fig 3b clearly shows that there are a few cavities on the surface of Ag NWs. With the increase of reaction time, particles form on the edge of cavities. These small particles agglomerate together to form larger clusters, and cavities are formed simultaneously. The porous hollow structure gradually formed, with the diameter increased slightly, and the surface becomes rougher.

2.1.3 Process analysis and mechanism discussion of galvanic replacement reaction

Because the standard electrode potential of Ag+/Ag（0.80V） is lower than that of $AuCl_4$-/Au (1.00V), when Ag NWs were added into $HAuCl_4$ solution, the displacement reaction between $AuCl_4$- and Ag take place spontaneously. The process can be regarded as the corrosion process of Ag NWs, in which Ag is oxidized to Ag+ and $AuCl_4$- is reduced to Au atoms. The chemical equation is as follows:

In the reaction, Ag NWs are electron sources and templates of gold nanotubes. Selective corrosion of the surface of Ag NWs plays an important role in the synthesis of Ag@Au hybrid nanotubes. The as-synthesized Ag NWs are coated by (100) longitudinally and (111) at the end. PVP covers the (100) surface, passivating the surface, and hinders the deposition of silver atoms on the surface. In the displacement reaction, the uncoated (111) crystal surface first reacts with $AuCl_4$- ions because of its high energy compared to (100). With the replacement reaction going on, the corroded surface of Ag NWs will be converted into surfaces with higher energy, which makes $AuCl_4$- ions more likely to react on these new surfaces, resulting in more $AuCl_4$- ions reducing to Au atoms at the sites where displacement reactions have taken place. The aggregation of these Au atoms leads to the grow of the particle size of gold nanoparticles. With the increase of reaction time, more surface silver atoms react with $AuCl_4$- further, and more Au atoms are formed to form new crystal nuclei. These nuclei grow up with the reaction to form gold nanoparticles, which leads to the increase of the density of gold nanoparticles. At the same time, due to the higher surface energy of the Ag NWs near the formed gold nanoparticles, more $AuCl_4$- ions are reduced to Au atoms near the original gold nanoparticles to form new crystal nuclei. With the further reaction, these new crystal nuclei and the original gold nanoparticles will grow up, leading to the aggregation of gold nanoparticles. From replacement reaction between Ag NWs and $AuCl_4$-, only one Au atom can be replaced by three Ag atoms. Therefore, with the progress of the reaction, the corrosion degree of Ag NWs is far greater than that of gold nanoparticles, and the hollow structure is gradually formed.

3 UV spectra, fluorescence excitation and emission spectra

Silver and gold nanoparticles exhibit surface plasmon resonance with a specific wavelength in the ultraviolet–visible region, and the plasma resonance wavelengths are different [14]. The surface plasmon resonance of Ag@Au hybrid nanotubes is characterized by the UV-Vis spectrum. Fig.5 shows the UV Vis spectra of the AgNWs substrate, and different Ag@Au hybrid nanotubes substrates. There are two characteristic peaks at 320 nm and 327 nm of AgNWs, and they corresponded to the quadrupole resonance and transverse plasmon resonance of nanowires, respectively. After the formation of Au nanoparticles, the characteristic peaks of UV Vis spectra of silver particles weaken or even disappear, and the broad peaks of gold nanoparticles appear at 520 nm, with the prolonging of reaction time, the UV-Vis spectrum the absorbance peaks redshift and become wider due to the increase of the number and volume of gold nanoparticles and the increase of the amount of gold of Ag@Au hybrid nanotubes.

One of the most important factors affecting the fluorescence enhancement effect is related to the coincidence degree of the excitation/ emission spectra of photoluminescent materials. The higher the coincidence degree is, the stronger the enhancement effect is. The ordered Ag@Au hybrid nanotubes have scattering or absorption characteristics will form their own plasma resonance peaks. Fig.6 shows the resonance spectra of ordered Ag@Au hybrid nanotubes, UV absorption spectrum, excitation spectrum and emission spectra of P3HT. The excitation peaks appear at 557 nm and 596 nm of P3HT on the ordered Ag@Au hybrid nanotubes. The maximum excitation wavelength of P3HT standard is 557nm; the emission spectrum of P3HT standard has two characteristic peaks at 665 nm and 726 nm respectively. The Ag@Au hybrid nanotubes have lager overlapped plasma resonance peaks than that of Ag nanowires at 557 nm. Therefore, 557 nm is selected as the excitation source for P3HT steady-state fluorescence experiment. The overlap part of plasma resonance peak at 520nm of the hybrid nanotubes with excitation spectrum P3HT is much larger than that of plasmon resonance peak at 320 nm of the hybrid nanotubes with emission spectrum P3HT, and the overlap part of plasmon resonance peak of the hybrid nanotubes with P3HT standard emission spectrum curve is very small, which indicates that it is ordered Ag@Au hybrid nanotubes. It is shown that the fluorescence enhancement effect of surface plasmon resonance on P3HT is mainly excitation enhancement.

4 Fluorescence effect of P3HT on different ordered Ag@Au hybrid nanotubes arrays

Fig. 7 shows fluorescence spectra of P3HT on different ordered Ag@Au hybrid nanotubes arrays. It can be seen that the fluorescence intensity of P3HT decreases with the increase of displacement reaction time. However, the fluorescence intensity of P3HT film on the ordered Ag@Au hybrid nanotubes arrays is still greater than that on the glass substrate, which indicates that the ordered Ag@Au hybrid nanotubes arrays can enhance the fluorescence effect of P3HT. After Ag NWs was replaced by gold nanoparticles on the surface of the ordered Ag@Au hybrid nanotubes arrays, the enhancement of the fluorescence of P3HT on t hybrid nanotubes arrays was weakened. The fluorescence intensity is reduced because three Ag atoms are consumed by the generation of one Au atom; the Ag atoms will be significantly lost. Moreover, the order of the Ag NWs arrays is destroyed with the displacement reaction, resulting in the further

decrease of the proportion of SPPs produced by the ordered Ag NWs. Moreover, with the displacement reaction, the order decreases with the displacement reaction, and the size and density of gold nanoparticles on the surface of Ag@Au hybrid nanotubes increase. The local plasmon resonance magnetic field generated by the gold nanoparticles and the ordered Ag NWs in Ag@Au hybrid nanotubes arrays is not matched, which leads to the poor coupling and propagation, and thus further reduced the surface local electromagnetic field of the hybrid nanotubes.

5 Raman effect of P3HT on different ordered Ag@Au hybrid nanotubes arrays

The change of morphology or chemical structure of fluorescence molecular on the metal surface will cause the change of Raman peak position. Fig. 8 shows the Raman spectra of P3HT on different ordered Ag@Au hybrid nanotubes arrays. There is no obvious change in the position of the Raman peaks of the P3HT on the hybrid nanotubes, which indicates that the existence of ordered Ag@Au hybrid nanotubes arrays does not change the structure or chemistry properties of P3HT film. The two strong Raman peaks at 1380 cm-1 and 1444 cm-1 are the stretching vibration of C-C skeleton and the stretching vibration of thiophene ring C-C of P3HT, respectively. The results show that the local electromagnetic field has a great influence on the Raman signal, the Raman signal of P3HT weakened, followed by the local electromagnetic field. The intensity of Raman signal of P3HT film on different ordered Ag@Au hybrid nanotubes arrays is obviously higher than that on the blank glass wafer, but the intensity of P3HT Raman signal decreases with the increase of reaction time, which indicates that the surface local electromagnetic field of the ordered Ag NWs is weakened after the displacement reaction, which is consistent with the above steady-state fluorescence spectra experimental results.

Conclusion

The galvanic displacement reaction is used to prepare ordered Ag@Au hybrid nanotubes at the expense of Ag NWs. The particle size and density of AuNP on the hybrid nanotubes can be adjusted by changing the reaction time of Ag NWs with $HAuCl_4$. Surface plasmon resonance property was measured by UV Vis spectra. The fluorescence intensity of P3HT on ordered Ag@Au hybrid nanotubes decrease with the degree of displacement reaction, which is due to the reduce of the local electromagnetic field after the displacement reaction. Even if the local electromagnetic field on the surface is weakened, the fluorescent intensity of P3HT on ordered Ag@Au hybrid nanotubes was also enhanced. The results show that the Ag@Au hybrid nanotubes arrays can effectively adjust the enhancement effect of surface plasmon resonance, and obtain the coupling effect differ from monometallic nanomaterials, which is expected to realize the tunable enhancement of the spectral properties of conjugated polymers.

References

[1] Olejnik M, Krajnik B, Kowalska D, et al. Imaging of fluorescence enhancement in photosynthetic complexes coupled to silver nanowires[J]. Applied Physics Letters, 2013, 102(8):136-4910.

[2] Guo SH, Britti DG, Heetderks JJ, et al. Spacer Layer Effect in Fluorescence Enhancement from Silver Nanowires over a Silver Film; Switching of Optimum Polarization[J]. Nano Letters, 2009, 9(7):2666–2670.

[3] Kim J, Han H, Kim Y H, et al. Au/Ag bilayered metal mesh as a si etching catalyst for controlled fabrication of si nanowires[J]. Acs Nano, 2011, 5(4):3222-3229.

[4] Gu X, Xu L, Fang T, et al. Au-Ag alloy nanoporous nanotubes[J]. Nano Research, 2009, 2(5):386-393.

[5] S Guan, X Fu, Y Tang, et al. AuAg@CdS double-walled nanotubes: synthesis and nonlinear absorption properties[J]. Nanoscale, 2017,9, 10277-10284

[6] Wang M, Wang M, Wang G , Su X. A fluorescence “off–on–off” sensing platform based on bimetallic gold/silver nanoclusters for ascorbate oxidase activity monitoring[J]. Analyst, 2020,145, 1001-1007

[7] hakraborti S, Basu RN, Panda SK. Vertically Aligned Silicon Nanowire Array Decorated by Ag or Au Nanoparticles as SERS Substrate for Bio-molecular Detection. Plasmonics, 2018, 13, 1057–1080.

[8] Kumeria T, Santos A, Losic D . Nanoporous Anodic Alumina Platforms: Engineered Surface Chemistry and Structure for Optical Sensing Applications[J]. Sensors, 2014, 14(7):11878-11918.

[9] Zhang Z, Ma C, He L, et al. Ultrafast synthesis of Au(I)-dodecanethiolate nanotubes for advanced Hg2+ sensor electrodes[J]. Nanoscale Res Lett, 2014, 9, 601.

[10] Sang H I, Yun T L, Wiley B, et al. Large-Scale Synthesis of Silver Nanocubes: The Role of HCl in Promoting Cube Perfection and Monodispersity[J]. Angewandte Chemie International Edition, 2005, 117(14): 2192-2195.

[11] Huang CC, Wei H J, Yeh Y C, et al. Injectable PLGA porous beads cellularized by hAFSCs for cellular cardiomyoplasty[J]. Biomaterials, 2012, 33(16):4069-4077.

[12] Pang B, Yang X, Xia Y. Putting gold nanocages to work for optical imaging, controlled release and cancer theranostics[J]. Nanomedicine, 2016, 11(13):1715-1728.

[13] Zhao M, Wang X, Yang X, et al. Hollow Metal Nanocrystals with Ultrathin, Porous Walls and Well-Controlled Surface Structures[J]. Advanced Materials, 2018, 30(48): 1801956.

[14] Lee K S , El-Sayed M A . Gold and Silver Nanoparticles in Sensing and Imaging: Sensitivity of Plasmon Response to Size, Shape, and Metal Composition[J]. Journal of Physical Chemistry B, 2006, 110(39):19220-19225.

Figures

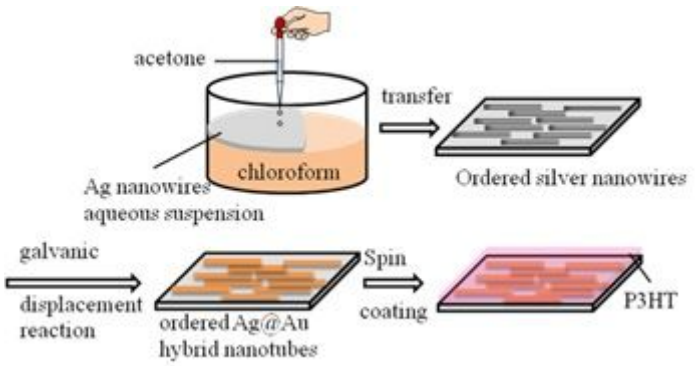

Figure 1

Schematic illustration of the fabrication process for ordered Ag@Au hybrid nanotubes films.

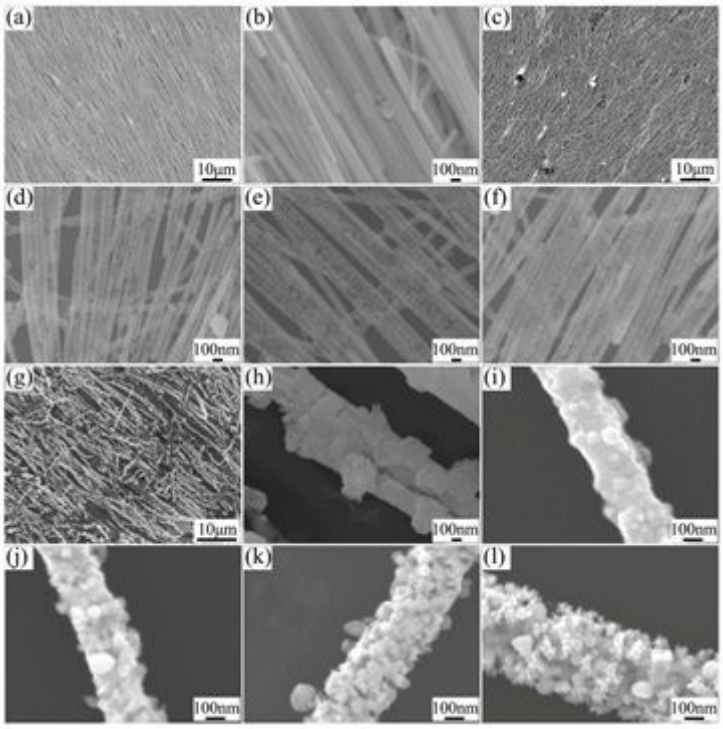

Figure 2

Scanning electron microscopy of ordered Ag NWs, and Ag@Au hybrid nanotubes((a, b) SEM images and magnified image of the ordered Ag NWs, (c-l) SEM images and magnified image of Ag@Au hybrid nanotubes.)

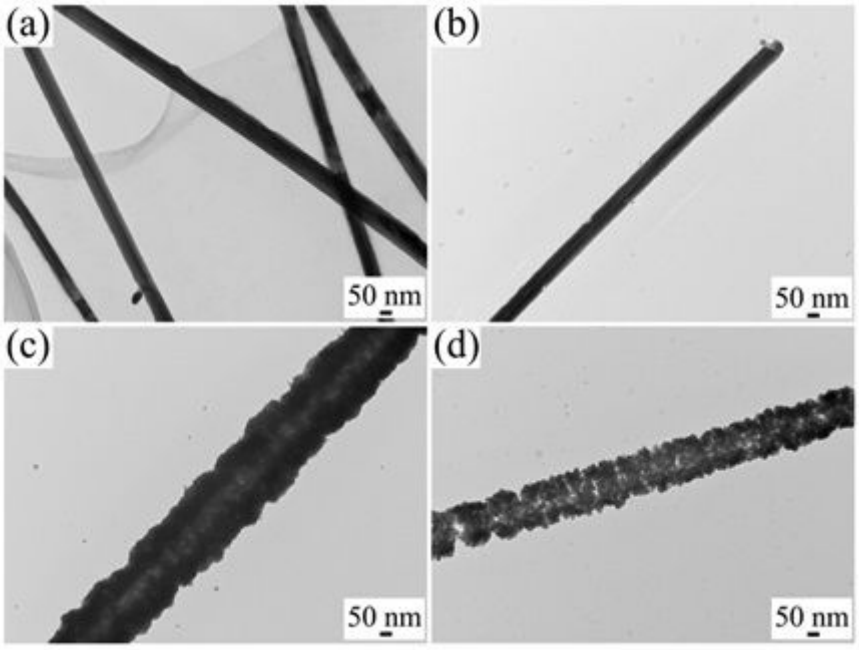

Figure 3

Transmission electron microscopy of Ag NWs, and different Ag@Au hybrid nanotubes(2.5, 5, 30min)

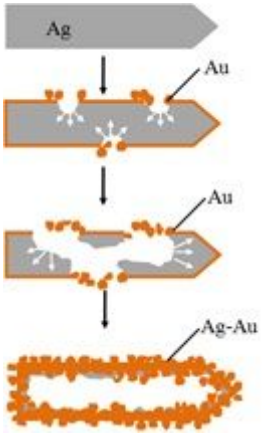

Figure 4

Process analysis and mechanism discussion of galvanic replacement reaction

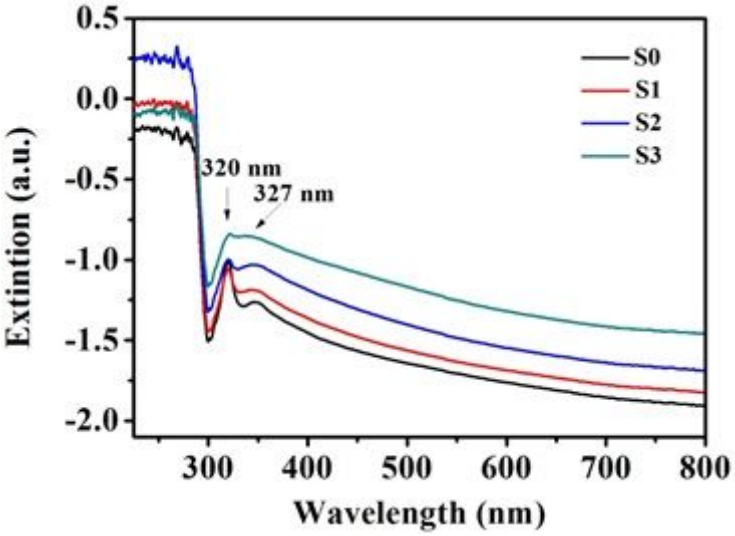

Figure 5

UV–vis extinction spectra of AgNWs substrate, and different Ag@Au hybrid nanotubes substrates

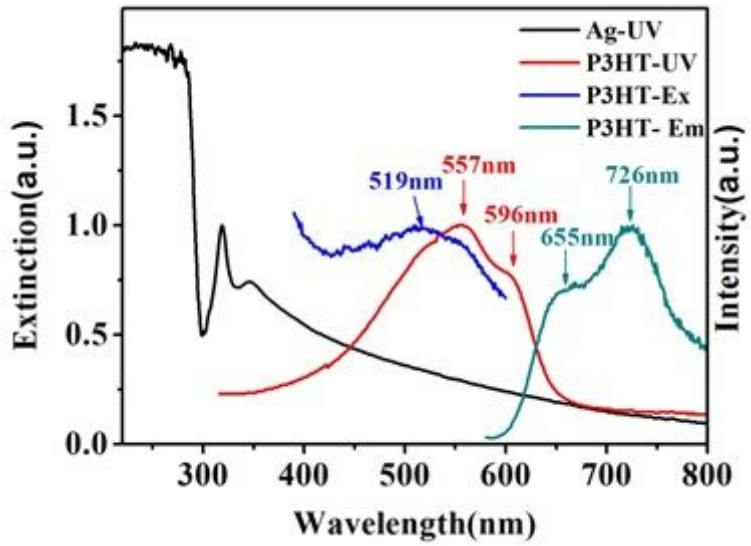

Figure 6

Extinction spectra of aligned AgNWs and P3HT films, and excitation and emission spectra P3HT film on quartz glass

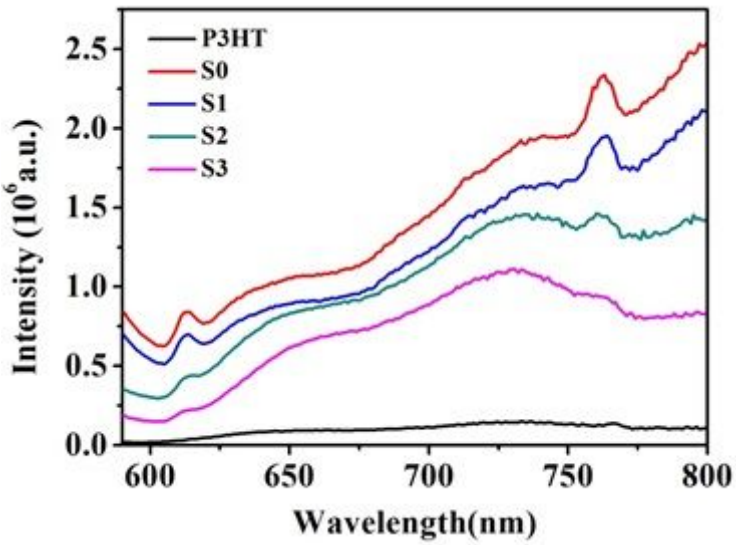

Figure 7

Fluorescence spectrum of P3HT on ordered AgNW and different Ag@Au hybrid nanotubes substrates

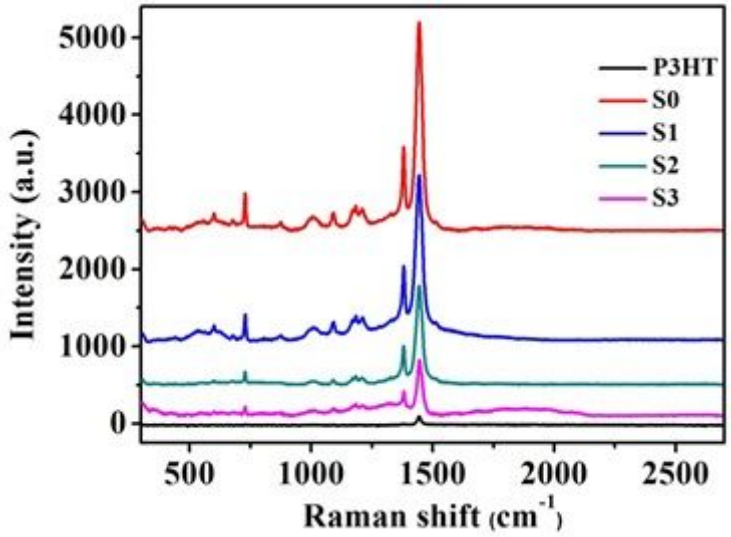

Figure 8

Raman spectra of the P3HT films on ordered AgNW and different Ag@Au hybrid nanotubes substrates